

Observation of the Doubly Cabibbo-Suppressed Decays $D^+ \rightarrow K^+\pi^0\pi^0$ and $D^+ \rightarrow K^+\pi^0\eta$

M. Ablikim¹, M. N. Achasov^{10,b}, P. Adlarson⁶⁸, S. Ahmed¹⁴, M. Albrecht⁴, R. Aliberti²⁸, A. Amoroso^{67A,67C}, M. R. An³², Q. An^{64,50}, X. H. Bai⁵⁸, Y. Bai⁴⁹, O. Bakina²⁹, R. Baldini Ferroli^{23A}, I. Balossino^{24A}, Y. Ban^{39,h}, K. Begzsuren²⁶, N. Berger²⁸, M. Bertani^{23A}, D. Bettoni^{24A}, F. Bianchi^{67A,67C}, J. Bloms⁶¹, A. Bortone^{67A,67C}, I. Boyko²⁹, R. A. Briere⁵, A. Brueggemann⁶¹, H. Cai⁶⁹, X. Cai^{1,50}, A. Calcaterra^{23A}, G. F. Cao^{1,55}, N. Cao^{1,55}, S. A. Cetin^{54A}, J. F. Chang^{1,50}, W. L. Chang^{1,55}, G. Chelkov^{29,a}, G. Chen¹, H. S. Chen^{1,55}, M. L. Chen^{1,50}, S. J. Chen³⁵, X. R. Chen²⁵, Y. B. Chen^{1,50}, Z. J. Chen^{20,i}, W. S. Cheng^{67C}, G. Cibinetto^{24A}, F. Cossio^{67C}, J. J. Cui⁴², H. L. Dai^{1,50}, J. P. Dai⁷¹, A. Dbeyssi¹⁴, R. E. de Boer⁴, D. Dedovich²⁹, Z. Y. Deng¹, A. Denig²⁸, I. Denysenko²⁹, M. Destefanis^{67A,67C}, F. De Mori^{67A,67C}, Y. Ding³³, J. Dong^{1,50}, L. Y. Dong^{1,55}, M. Y. Dong^{1,50,55}, X. Dong⁶⁹, S. X. Du⁷³, Y. L. Fan⁶⁹, J. Fang^{1,50}, S. S. Fang^{1,55}, Y. Fang¹, R. Farinelli^{24A}, L. Fava^{67B,67C}, F. Feldbauer⁴, G. Felici^{23A}, C. Q. Feng^{64,50}, J. H. Feng⁵¹, M. Fritsch⁴, C. D. Fu¹, Y. N. Gao^{39,h}, Yang Gao^{64,50}, I. Garzia^{24A,24B}, P. T. Ge⁶⁹, C. Geng⁵¹, E. M. Gersabeck⁵⁹, A. Gilman⁶², K. Goetzen¹¹, L. Gong³³, W. X. Gong^{1,50}, W. Gradl²⁸, M. Greco^{67A,67C}, L. M. Gu³⁵, M. H. Gu^{1,50}, C. Y. Guan^{1,55}, A. Q. Guo²⁵, A. Q. Guo²², L. B. Guo³⁴, R. P. Guo⁴¹, Y. P. Guo^{9,g}, A. Guskov^{29,a}, T. T. Han⁴², W. Y. Han³², X. Q. Hao¹⁵, F. A. Harris⁵⁷, K. L. He^{1,55}, F. H. Heinsius⁴, C. H. Heinz²⁸, Y. K. Heng^{1,50,55}, C. Herold⁵², M. Himmelreich^{11,e}, T. Holtmann⁴, G. Y. Hou^{1,55}, Y. R. Hou⁵⁵, Z. L. Hou¹, H. M. Hu^{1,55}, J. F. Hu^{48,j}, T. Hu^{1,50,55}, Y. Hu¹, G. S. Huang^{64,50}, L. Q. Huang⁶⁵, X. T. Huang⁴², Y. P. Huang¹, Z. Huang^{39,h}, T. Hussain⁶⁶, N. Hüsken^{22,28}, W. Imoehl²², M. Irshad^{64,50}, S. Jaeger⁴, S. Janchiv²⁶, Q. Ji¹, Q. P. Ji¹⁵, X. B. Ji^{1,55}, X. L. Ji^{1,50}, Y. Y. Ji⁴², H. B. Jiang⁴², X. S. Jiang^{1,50,55}, J. B. Jiao⁴², Z. Jiao¹⁸, S. Jin³⁵, Y. Jin⁵⁸, M. Q. Jing^{1,55}, T. Johansson⁶⁸, N. Kalantar-Nayestanaki⁵⁶, X. S. Kang³³, R. Kappert⁵⁶, M. Kavatsyuk⁵⁶, B. C. Ke⁷³, I. K. Keshk⁴, A. Khoukaz⁶¹, P. Kiese²⁸, R. Kiuchi¹, R. Kliemt¹¹, L. Koch³⁰, O. B. Kolcu^{54A}, B. Kopf⁴, M. Kuemmel⁴, M. Kuessner⁴, A. Kupsc^{37,68}, W. Kühn³⁰, J. J. Lane⁵⁹, J. S. Lange³⁰, P. Larin¹⁴, A. Lavania²¹, L. Lavezzi^{67A,67C}, Z. H. Lei^{64,50}, H. Leithoff²⁸, M. Lellmann²⁸, T. Lenz²⁸, C. Li⁴⁰, C. H. Li³², Cheng Li^{64,50}, D. M. Li⁷³, F. Li^{1,50}, G. Li¹, H. Li^{64,50}, H. Li⁴⁴, H. B. Li^{1,55}, H. J. Li¹⁵, H. N. Li^{48,j}, J. L. Li⁴², J. Q. Li⁴, J. S. Li⁵¹, Ke Li¹, L. K. Li¹, Lei Li³, P. R. Li^{31,k,l}, S. Y. Li⁵³, T. Li⁴², W. D. Li^{1,55}, W. G. Li¹, X. H. Li^{64,50}, X. L. Li⁴², Xiaoyu Li^{1,55}, Z. Y. Li⁵¹, H. Liang²⁷, H. Liang^{1,55}, H. Liang^{64,50}, Y. F. Liang⁴⁶, Y. T. Liang²⁵, G. R. Liao¹², J. Libby²¹, A. Limphirat⁵², C. X. Lin⁵¹, D. X. Lin²⁵, T. Lin¹, B. J. Liu¹, C. X. Liu¹, D. Liu^{14,64}, F. H. Liu⁴⁵, Fang Liu¹, Feng Liu⁶, G. M. Liu^{48,j}, H. M. Liu^{1,55}, Huanhuan Liu¹, Huihui Liu¹⁶, J. B. Liu^{64,50}, J. L. Liu⁶⁵, J. Y. Liu^{1,55}, K. Liu¹, K. Y. Liu³³, Ke Liu¹⁷, L. Liu^{64,50}, M. H. Liu^{9,g}, P. L. Liu¹, Q. Liu⁵⁵, Q. Liu⁶⁹, S. B. Liu^{64,50}, T. Liu^{9,g}, W. M. Liu^{64,50}, X. Liu^{31,k,l}, Y. Liu^{31,k,l}, Y. B. Liu³⁶, Z. A. Liu^{1,50,55}, Z. Q. Liu⁴², X. C. Lou^{1,50,55}, F. X. Lu⁵¹, H. J. Lu¹⁸, J. G. Lu^{1,50}, X. L. Lu¹, Y. Lu¹, Y. P. Lu^{1,50}, C. L. Luo³⁴, M. X. Luo⁷², T. Luo^{9,g}, X. L. Luo^{1,50}, X. R. Lyu⁵⁵, F. C. Ma³³, H. L. Ma¹, L. L. Ma⁴², M. M. Ma^{1,55}, Q. M. Ma¹, R. Q. Ma^{1,55}, R. T. Ma⁵⁵, X. Y. Ma^{1,50}, Y. Ma^{39,h}, F. E. Maas¹⁴, M. Maggiora^{67A,67C}, S. Maldaner⁴, S. Malde⁶², Q. A. Malik⁶⁶, A. Mangoni^{23B}, Y. J. Mao^{39,h}, Z. P. Mao¹, S. Marcello^{67A,67C}, Z. X. Meng⁵⁸, J. G. Messchendorp^{56,d}, G. Mezzadri^{24A}, T. J. Min³⁵, R. E. Mitchell²², X. H. Mo^{1,50,55}, N. Yu. Muchnoi^{10,b}, H. Muramatsu⁶⁰, S. Nakhoul^{11,e}, Y. Nefedov²⁹, F. Nerling^{11,e}, I. B. Nikolaev^{10,b}, Z. Ning^{1,50}, S. Nisar^{8,m}, S. L. Olsen⁵⁵, Q. Ouyang^{1,50,55}, S. Pacetti^{23B,23C}, X. Pan^{9,g}, Y. Pan⁵⁹, A. Pathak¹, A. Pathak²⁷, P. Patteri^{23A}, M. Pelizaeus⁴, H. P. Peng^{64,50}, K. Peters^{11,e}, J. Pettersson⁶⁸, J. L. Ping³⁴, R. G. Ping^{1,55}, S. Pogodin²⁹, R. Poling⁶⁰, V. Prasad^{64,50}, H. Qi^{64,50}, H. R. Qi⁵³, M. Qi³⁵, T. Y. Qi^{9,g}, S. Qian^{1,50}, W. B. Qian⁵⁵, Z. Qian⁵¹, C. F. Qiao⁵⁵, J. J. Qin⁶⁵, L. Q. Qin¹², X. P. Qin^{9,g}, X. S. Qin⁴², Z. H. Qin^{1,50}, J. F. Qiu¹, S. Q. Qu³⁶, S. Q. Qu⁵³, K. H. Rashid⁶⁶, K. Ravindran²¹, C. F. Redmer²⁸, A. Rivetti^{67C}, V. Rodin⁵⁶, M. Rolo^{67C}, G. Rong^{1,55}, Ch. Rosner¹⁴, M. Rump⁶¹, H. S. Sang⁶⁴, A. Sarantsev^{29,c}, Y. Schelhaas²⁸, C. Schnier⁴, K. Schoenning⁶⁸, M. Scodeggio^{24A,24B}, W. Shan¹⁹, X. Y. Shan^{64,50}, J. F. Shangguan⁴⁷, M. Shao^{64,50}, C. P. Shen^{9,g}, H. F. Shen^{1,55}, X. Y. Shen^{1,55}, H. C. Shi^{64,50}, R. S. Shi^{1,55}, X. Shi^{1,50}, X. D. Shi^{64,50}, J. J. Song¹⁵, W. M. Song^{27,1}, Y. X. Song^{39,h}, S. Sosio^{67A,67C}, S. Spataro^{67A,67C}, K. X. Su⁶⁹, P. P. Su⁴⁷, G. X. Sun¹, H. K. Sun¹, J. F. Sun¹⁵, L. Sun⁶⁹, S. S. Sun^{1,55}, T. Sun^{1,55}, W. Y. Sun²⁷, X. Sun^{20,i}, Y. J. Sun^{64,50}, Y. Z. Sun¹, Z. T. Sun⁴², Y. H. Tan⁶⁹, Y. X. Tan^{64,50}, C. J. Tang⁴⁶, G. Y. Tang¹, J. Tang⁵¹, J. X. Teng^{64,50}, V. Thoren⁶⁸, W. H. Tian⁴⁴, Y. T. Tian²⁵, I. Uman^{54B}, B. Wang¹, C. W. Wang³⁵, D. Y. Wang^{39,h}, H. J. Wang^{31,k,l}, H. P. Wang^{1,55}, K. Wang^{1,50}, L. L. Wang¹, M. Wang⁴², M. Z. Wang^{39,h}, Meng Wang^{1,55}, S. Wang^{9,g}, W. Wang⁵¹, W. H. Wang⁶⁹, W. P. Wang^{64,50}, X. Wang^{39,h}, X. F. Wang^{31,k,l}, X. L. Wang^{9,g}, Y. D. Wang³⁸, Y. F. Wang^{1,50,55},

Y. Q. Wang¹, Y. Y. Wang^{31,k,l}, Ying Wang⁵¹, Z. Wang^{1,50}, Z. Y. Wang¹, Ziyi Wang⁵⁵, D. H. Wei¹², F. Weidner⁶¹, S. P. Wen¹, D. J. White⁵⁹, U. Wiedner⁴, G. Wilkinson⁶², M. Wolke⁶⁸, L. Wollenberg⁴, J. F. Wu^{1,55}, L. H. Wu¹, L. J. Wu^{1,55}, X. Wu^{9,g}, X. H. Wu²⁷, Y. Wu⁶⁴, Z. Wu^{1,50}, L. Xia^{64,50}, T. Xiang^{39,h}, H. Xiao^{9,g}, S. Y. Xiao¹, Z. J. Xiao³⁴, X. H. Xie^{39,h}, Y. G. Xie^{1,50}, Y. H. Xie⁶, Z. P. Xie^{64,50}, T. Y. Xing^{1,55}, C. J. Xu⁵¹, G. F. Xu¹, Q. J. Xu¹³, S. Y. Xu⁶³, X. P. Xu⁴⁷, Y. C. Xu⁵⁵, F. Yan^{9,g}, L. Yan^{9,g}, W. B. Yan^{64,50}, W. C. Yan⁷³, H. J. Yang^{43,f}, H. X. Yang¹, L. Yang⁴⁴, S. L. Yang⁵⁵, Yifan Yang^{1,55}, Zhi Yang²⁵, M. Ye^{1,50}, M. H. Ye⁷, J. H. Yin¹, Z. Y. You⁵¹, B. X. Yu^{1,50,55}, C. X. Yu³⁶, G. Yu^{1,55}, J. S. Yu^{20,i}, T. Yu⁶⁵, C. Z. Yuan^{1,55}, L. Yuan², X. Q. Yuan^{39,h}, Y. Yuan^{1,55}, Z. Y. Yuan⁵¹, C. X. Yue³², A. A. Zafar⁶⁶, X. Zeng Zeng⁶, Y. Zeng^{20,i}, A. Q. Zhang¹, B. X. Zhang¹, G. Y. Zhang¹⁵, H. Zhang⁶⁴, H. H. Zhang²⁷, H. H. Zhang⁵¹, H. Y. Zhang^{1,50}, J. L. Zhang⁷⁰, J. Q. Zhang³⁴, J. W. Zhang^{1,50,55}, J. Y. Zhang¹, J. Z. Zhang^{1,55}, Jianyu Zhang^{1,55}, Jiawei Zhang^{1,55}, L. M. Zhang⁵³, L. Q. Zhang⁵¹, Lei Zhang³⁵, S. F. Zhang³⁵, Shulei Zhang^{20,i}, X. D. Zhang³⁸, X. Y. Zhang⁴², Y. Zhang⁶², Y. T. Zhang⁷³, Y. H. Zhang^{1,50}, Yan Zhang^{64,50}, Yao Zhang¹, Z. Y. Zhang⁶⁹, G. Zhao¹, J. Zhao³², J. Y. Zhao^{1,55}, J. Z. Zhao^{1,50}, Lei Zhao^{64,50}, Ling Zhao¹, M. G. Zhao³⁶, Q. Zhao¹, S. J. Zhao⁷³, Y. B. Zhao^{1,50}, Y. X. Zhao²⁵, Z. G. Zhao^{64,50}, A. Zhemchugov^{29,a}, B. Zheng⁶⁵, J. P. Zheng^{1,50}, Y. H. Zheng⁵⁵, B. Zhong³⁴, C. Zhong⁶⁵, L. P. Zhou^{1,55}, X. Zhou⁶⁹, X. K. Zhou⁵⁵, X. R. Zhou^{64,50}, X. Y. Zhou³², J. Zhu³⁶, K. Zhu¹, K. J. Zhu^{1,50,55}, S. H. Zhu⁶³, T. J. Zhu⁷⁰, W. J. Zhu^{9,g}, W. J. Zhu³⁶, Y. C. Zhu^{64,50}, Z. A. Zhu^{1,55}, B. S. Zou¹, J. H. Zou¹

(BESIII Collaboration)

¹ *Institute of High Energy Physics, Beijing 100049, People's Republic of China*

² *Beihang University, Beijing 100191, People's Republic of China*

³ *Beijing Institute of Petrochemical Technology, Beijing 102617, People's Republic of China*

⁴ *Bochum Ruhr-University, D-44780 Bochum, Germany*

⁵ *Carnegie Mellon University, Pittsburgh, Pennsylvania 15213, USA*

⁶ *Central China Normal University, Wuhan 430079, People's Republic of China*

⁷ *China Center of Advanced Science and Technology, Beijing 100190, People's Republic of China*

⁸ *COMSATS University Islamabad, Lahore Campus, Defence Road, Off Raiwind Road, 54000 Lahore, Pakistan*

⁹ *Fudan University, Shanghai 200433, People's Republic of China*

¹⁰ *G.I. Budker Institute of Nuclear Physics SB RAS (BINP), Novosibirsk 630090, Russia*

¹¹ *GSI Helmholtzcentre for Heavy Ion Research GmbH, D-64291 Darmstadt, Germany*

¹² *Guangxi Normal University, Guilin 541004, People's Republic of China*

¹³ *Hangzhou Normal University, Hangzhou 310036, People's Republic of China*

¹⁴ *Helmholtz Institute Mainz, Staudinger Weg 18, D-55099 Mainz, Germany*

¹⁵ *Henan Normal University, Xinxiang 453007, People's Republic of China*

¹⁶ *Henan University of Science and Technology, Luoyang 471003, People's Republic of China*

¹⁷ *Henan University of Technology, Zhengzhou 450001, People's Republic of China*

¹⁸ *Huangshan College, Huangshan 245000, People's Republic of China*

¹⁹ *Hunan Normal University, Changsha 410081, People's Republic of China*

²⁰ *Hunan University, Changsha 410082, People's Republic of China*

²¹ *Indian Institute of Technology Madras, Chennai 600036, India*

²² *Indiana University, Bloomington, Indiana 47405, USA*

²³ *INFN Laboratori Nazionali di Frascati, (A)INFN Laboratori Nazionali di Frascati, I-00044, Frascati, Italy; (B)INFN Sezione di Perugia, I-06100, Perugia, Italy; (C)University of Perugia, I-06100, Perugia, Italy*

²⁴ *INFN Sezione di Ferrara, (A)INFN Sezione di Ferrara, I-44122, Ferrara, Italy; (B)University of Ferrara, I-44122, Ferrara, Italy*

²⁵ *Institute of Modern Physics, Lanzhou 730000, People's Republic of China*

²⁶ *Institute of Physics and Technology, Peace Ave. 54B, Ulaanbaatar 13330, Mongolia*

²⁷ *Jilin University, Changchun 130012, People's Republic of China*

²⁸ *Johannes Gutenberg University of Mainz, Johann-Joachim-Becher-Weg 45, D-55099 Mainz, Germany*

²⁹ *Joint Institute for Nuclear Research, 141980 Dubna, Moscow region, Russia*

³⁰ *Justus-Liebig-Universitaet Giessen, II. Physikalisches Institut, Heinrich-Buff-Ring 16, D-35392 Giessen, Germany*

³¹ *Lanzhou University, Lanzhou 730000, People's Republic of China*

³² *Liaoning Normal University, Dalian 116029, People's Republic of China*

- ³³ *Liaoning University, Shenyang 110036, People's Republic of China*
- ³⁴ *Nanjing Normal University, Nanjing 210023, People's Republic of China*
- ³⁵ *Nanjing University, Nanjing 210093, People's Republic of China*
- ³⁶ *Nankai University, Tianjin 300071, People's Republic of China*
- ³⁷ *National Centre for Nuclear Research, Warsaw 02-093, Poland*
- ³⁸ *North China Electric Power University, Beijing 102206, People's Republic of China*
- ³⁹ *Peking University, Beijing 100871, People's Republic of China*
- ⁴⁰ *Qufu Normal University, Qufu 273165, People's Republic of China*
- ⁴¹ *Shandong Normal University, Jinan 250014, People's Republic of China*
- ⁴² *Shandong University, Jinan 250100, People's Republic of China*
- ⁴³ *Shanghai Jiao Tong University, Shanghai 200240, People's Republic of China*
- ⁴⁴ *Shanxi Normal University, Linfen 041004, People's Republic of China*
- ⁴⁵ *Shanxi University, Taiyuan 030006, People's Republic of China*
- ⁴⁶ *Sichuan University, Chengdu 610064, People's Republic of China*
- ⁴⁷ *Soochow University, Suzhou 215006, People's Republic of China*
- ⁴⁸ *South China Normal University, Guangzhou 510006, People's Republic of China*
- ⁴⁹ *Southeast University, Nanjing 211100, People's Republic of China*
- ⁵⁰ *State Key Laboratory of Particle Detection and Electronics, Beijing 100049, Hefei 230026, People's Republic of China*
- ⁵¹ *Sun Yat-Sen University, Guangzhou 510275, People's Republic of China*
- ⁵² *Suranaree University of Technology, University Avenue 111, Nakhon Ratchasima 30000, Thailand*
- ⁵³ *Tsinghua University, Beijing 100084, People's Republic of China*
- ⁵⁴ *Turkish Accelerator Center Particle Factory Group, (A)Istinye University, 34010, Istanbul, Turkey; (B)Near East University, Nicosia, North Cyprus, Mersin 10, Turkey*
- ⁵⁵ *University of Chinese Academy of Sciences, Beijing 100049, People's Republic of China*
- ⁵⁶ *University of Groningen, NL-9747 AA Groningen, The Netherlands*
- ⁵⁷ *University of Hawaii, Honolulu, Hawaii 96822, USA*
- ⁵⁸ *University of Jinan, Jinan 250022, People's Republic of China*
- ⁵⁹ *University of Manchester, Oxford Road, Manchester, M13 9PL, United Kingdom*
- ⁶⁰ *University of Minnesota, Minneapolis, Minnesota 55455, USA*
- ⁶¹ *University of Muenster, Wilhelm-Klemm-Str. 9, 48149 Muenster, Germany*
- ⁶² *University of Oxford, Keble Rd, Oxford, UK OX13RH*
- ⁶³ *University of Science and Technology Liaoning, Anshan 114051, People's Republic of China*
- ⁶⁴ *University of Science and Technology of China, Hefei 230026, People's Republic of China*
- ⁶⁵ *University of South China, Hengyang 421001, People's Republic of China*
- ⁶⁶ *University of the Punjab, Lahore-54590, Pakistan*
- ⁶⁷ *University of Turin and INFN, (A)University of Turin, I-10125, Turin, Italy; (B)University of Eastern Piedmont, I-15121, Alessandria, Italy; (C)INFN, I-10125, Turin, Italy*
- ⁶⁸ *Uppsala University, Box 516, SE-75120 Uppsala, Sweden*
- ⁶⁹ *Wuhan University, Wuhan 430072, People's Republic of China*
- ⁷⁰ *Xinyang Normal University, Xinyang 464000, People's Republic of China*
- ⁷¹ *Yunnan University, Kunming 650500, People's Republic of China*
- ⁷² *Zhejiang University, Hangzhou 310027, People's Republic of China*
- ⁷³ *Zhengzhou University, Zhengzhou 450001, People's Republic of China*
- ^a *Also at the Moscow Institute of Physics and Technology, Moscow 141700, Russia*
- ^b *Also at the Novosibirsk State University, Novosibirsk, 630090, Russia*
- ^c *Also at the NRC "Kurchatov Institute", PNPI, 188300, Gatchina, Russia*
- ^d *Currently at Istanbul Arel University, 34295 Istanbul, Turkey*
- ^e *Also at Goethe University Frankfurt, 60323 Frankfurt am Main, Germany*
- ^f *Also at Key Laboratory for Particle Physics, Astrophysics and Cosmology, Ministry of Education; Shanghai Key Laboratory for Particle Physics and Cosmology; Institute*

of Nuclear and Particle Physics, Shanghai 200240, People's Republic of China

^g Also at Key Laboratory of Nuclear Physics and Ion-beam Application (MOE) and Institute of Modern Physics, Fudan University, Shanghai 200443, People's Republic of China

^h Also at State Key Laboratory of Nuclear Physics and Technology, Peking University, Beijing 100871, People's Republic of China

ⁱ Also at School of Physics and Electronics, Hunan University, Changsha 410082, China

^j Also at Guangdong Provincial Key Laboratory of Nuclear Science, Institute of Quantum Matter, South China Normal University, Guangzhou 510006, China

^k Also at Frontiers Science Center for Rare Isotopes, Lanzhou University, Lanzhou 730000, People's Republic of China

^l Also at Lanzhou Center for Theoretical Physics, Lanzhou University, Lanzhou 730000, People's Republic of China

^m Also at the Department of Mathematical Sciences, IBA, Karachi, Pakistan

By analyzing e^+e^- annihilation data corresponding to an integrated luminosity of 2.93 fb^{-1} collected at the center-of-mass energy of 3.773 GeV with the BESIII detector, we report the first observations of the doubly Cabibbo-suppressed decays $D^+ \rightarrow K^+\pi^0\pi^0$ and $D^+ \rightarrow K^+\pi^0\eta$. The branching fractions of $D^+ \rightarrow K^+\pi^0\pi^0$ and $D^+ \rightarrow K^+\pi^0\eta$ are measured to be $(2.1 \pm 0.4_{\text{stat}} \pm 0.1_{\text{syst}}) \times 10^{-4}$ and $(2.1 \pm 0.6_{\text{stat}} \pm 0.1_{\text{syst}}) \times 10^{-4}$ with statistical significances of 8.0σ and 5.0σ , respectively. In addition, we search for the subprocesses $D^+ \rightarrow K^*(892)^+\pi^0$ and $D^+ \rightarrow K^*(892)^+\eta$ with $K^*(892)^+ \rightarrow K^+\pi^0$. The branching fraction of $D^+ \rightarrow K^*(892)^+\eta$ is determined to be $(4.7^{+1.9}_{-1.6_{\text{stat}}} \pm 0.2_{\text{syst}}) \times 10^{-4}$, with a statistical significance of 3.3σ . No significant signal for $D^+ \rightarrow K^*(892)^+\pi^0$ is found and we set an upper limit on the branching fraction of this decay at the 90% confidence level to be 4.5×10^{-4} .

To date, only a few doubly Cabibbo-suppressed (DCS) decays of the charmed D^0 , D^+ , and D_s^+ mesons and the charmed Λ_c^+ baryon have been observed [1]. Naively, the branching fractions (BFs) of DCS decays are expected to be suppressed relative to their Cabibbo-favored (CF) counterparts by a factor on the order of $(0.5 - 2.0) \tan^4 \theta_C$, where θ_C is the Cabibbo mixing angle and $\tan^4 \theta_C = 0.29\%$. This ratio currently holds for most known DCS decays. One notable exception is in the decay $D^+ \rightarrow K^+\pi^+\pi^-\pi^0$, which was recently observed at BESIII [2]. The ratio of the branching fraction of the DCS decay $D^+ \rightarrow K^+\pi^+\pi^-\pi^0$ relative to the CF decay $D^+ \rightarrow K^-\pi^+\pi^+\pi^0$ was determined to be $(6.3 \pm 0.5) \tan^4 \theta_C$, which is significantly larger than expectations. This anomalous ratio was later confirmed in an independent measurement at BESIII [3]. Therefore, observation of more DCS decays of charmed mesons and determination of their decay BFs offers critical complementary information required to investigate such anomalous behavior.

In addition, the BFs of two-body hadronic D decays have been the subject of several recent theoretical calculations, both with and without incorporating SU(3) flavor symmetry breaking effects, as well as calculations focused on charge-parity (CP) violation [4–11]. For example, the BF of the decay $D^+ \rightarrow K^{*+}\pi^0(\eta)$ is predicted to be on the order of 10^{-4} using the pole model [5], the factorization assisted topological-amplitude (FAT) approach [7], and the diagrammatic approach [8], with results differing from each other by a factor of two. Experimental knowledge, however, of DCS decays of the form $D \rightarrow VP$, where V is a vector and P a pseudoscalar meson, is still rather scarce. Measurements

of the BFs of these decays provide crucial tests to various theoretical predictions, thereby aiding our understanding of SU(3) flavor symmetry breaking effects, and further improving theoretical calculations of CP violation in the charm sector. Throughout the text, charge conjugated decays are always implied and K^{*+} denotes $K^*(892)^+$.

This Letter reports the first measurements of the DCS decays $D^+ \rightarrow K^+\pi^0\pi^0$ and $D^+ \rightarrow K^+\pi^0\eta$ as well as the first searches for $D^+ \rightarrow K^{*+}\pi^0$ and $D^+ \rightarrow K^{*+}\eta$. Because of their low background contamination, the decay $D^+ \rightarrow K^+\pi^0\pi^0(\eta)$ offers an ideal opportunity to access the subprocess $D^+ \rightarrow K^{*+}\pi^0(\eta)$ with $K^{*+} \rightarrow K^+\pi^0$. The related DCS decay $D^+ \rightarrow K^0\pi^+\pi^0(\eta)$, on the other hand, suffers from large backgrounds from the CF decay $D^+ \rightarrow \bar{K}^0\pi^+\pi^0(\eta)$.

This analysis is based on 2.93 fb^{-1} of e^+e^- annihilation data [12] taken with the BESIII detector at the center-of-mass energy $\sqrt{s} = 3.773 \text{ GeV}$. This energy point is above the threshold to produce $D\bar{D}$ and below that to produce $D^*\bar{D}$, the D and \bar{D} mesons are produced in pairs with no additional hadrons, where D and D^* denote charged or neutral charmed meson and their excited states, respectively.

Details about the design and performance of the BESIII detector are given in Refs. [13]. Simulated samples produced with a GEANT4-based [14] Monte Carlo (MC) simulation, which includes the geometric description of the BESIII detector and the detector response, are used to determine the detection efficiency and to estimate backgrounds. The simulation includes the beam energy spread and initial state radiation (ISR) in the e^+e^- annihilations modeled with the generator KKMC [15]. The signal of $D^+ \rightarrow K^+\pi^0\pi^0(\eta)$ is simulated

using an MC generator that incorporates the resonant decay $D^+ \rightarrow K^{*+}\pi^0(\eta)$ and the phase space decay $D^+ \rightarrow K^+\pi^0\pi^0(\eta)$. The background is studied using an inclusive MC sample that consists of the production of $D\bar{D}$ pairs with consideration of quantum coherence for all neutral D modes, the non- $D\bar{D}$ decays of the $\psi(3770)$, the ISR production of the J/ψ and $\psi(3686)$ states, and the continuum processes incorporated in KKMC [15]. The known decay modes are modeled with EVTGEN [16] using the corresponding BFs taken from the Particle Data Group [1], while the remaining unknown decays from the charmonium states are modeled with LUNDCHARM [17]. Final state radiation from charged final state particles is incorporated using PHOTOS [18].

The BFs of the signal decays are measured with a double-tag technique that was first developed by the Mark III Collaboration [19]. Signal D^+ decays are reconstructed alongside hadronic D^- decays to $K^+\pi^-\pi^-$ or $K_S^0\pi^-$, which have high yields and cleanest tag environments thereby give better signal significances. The fully reconstructed D^- is called the single-tag (ST) meson. Events in which both the signal D^+ meson and the ST D^- meson are found are called double-tag (DT) events. For a given signal decay, the decay BF is determined by

$$\mathcal{B}_{\text{sig}} = N_{\text{DT}} / \sum_{i=1}^2 [N_{\text{ST}}^i (\epsilon_{\text{DT}}^i / \epsilon_{\text{ST}}^i)], \quad (1)$$

where N_{DT} is the yield of DT events, ϵ_{DT} is the efficiency of selecting a DT event, N_{ST} and ϵ_{ST} are the yield and corresponding selection efficiency of the ST D^- mesons, and i stands for tag modes.

Candidate K_S^0 , π^0 , and η mesons are formed via the decays $K_S^0 \rightarrow \pi^+\pi^-$, $\pi^0 \rightarrow \gamma\gamma$, and $\eta \rightarrow \gamma\gamma$. The K^\pm , π^\pm , K_S^0 , π^0 , and η candidates are reconstructed and identified using the same criteria as in Refs. [2, 20–29].

The ST D^- mesons are distinguished from combinatorial backgrounds using two kinematic variables: the energy difference $\Delta E_{\text{tag}} \equiv E_{D^-} - E_b$ and the beam-constrained mass $M_{\text{BC}}^{\text{tag}} \equiv \sqrt{E_b^2 - |\vec{p}_{D^-}|^2}$. Here, E_b is the beam energy, and \vec{p}_{D^-} and E_{D^-} are the momentum and energy, respectively, of the D^- candidate in the rest frame of the e^+e^- system. If more than one candidate survives the selection criteria of a given tag mode, the combination with the minimum $|\Delta E_{\text{tag}}|$ is chosen. Tagged D^- candidates are selected with a requirement of $\Delta E_{\text{tag}} \in (-25, 25)$ MeV to suppress combinatorial backgrounds in the $M_{\text{BC}}^{\text{tag}}$ distributions. To extract the number of ST D^- mesons for each tag mode, maximum likelihood fits have been performed on the individual $M_{\text{BC}}^{\text{tag}}$ distributions [2, 20–29]. The number of ST D^- mesons summed over the two tag modes is $N_{\text{ST}} = (892.2 \pm 1.1_{\text{stat}}) \times 10^3$.

Candidates for the DCS D^+ decays are selected with

the residual neutral and charged particles not used in the D^- tag reconstruction. Similar to the tag side, the energy difference and beam-constrained mass of the signal side, ΔE_{sig} and $M_{\text{BC}}^{\text{sig}}$, respectively, are calculated. For each signal decay, if there are multiple combinations, the one giving the minimum $|\Delta E_{\text{sig}}|$ is kept. The accepted candidates are required to fall in the intervals $\Delta E_{\text{sig}} \in (-78, 36)$ MeV and $\Delta E_{\text{sig}} \in (-52, 31)$ MeV for $D^+ \rightarrow K^+\pi^0\pi^0$ and $D^+ \rightarrow K^+\pi^0\eta$, respectively. To reduce background events from non- D^+D^- processes, the minimum opening angle between the D^+ and D^- must be greater than 167° . This requirement suppresses 57% (79%) of background for $D^+ \rightarrow K^+\pi^0\pi^0(\eta)$ at the cost of losing 9% of the two signal decays. For $D^+ \rightarrow K^+\pi^0\pi^0$, the invariant mass of the $\pi^0\pi^0$ combination is required to be outside (0.388, 0.588) GeV/ c^2 to reject the dominant background from the singly Cabibbo-suppressed decay $D^+ \rightarrow K^+K_S^0(\rightarrow \pi^0\pi^0)$.

The resulting distributions of $M_{\text{BC}}^{\text{tag}}$ versus $M_{\text{BC}}^{\text{sig}}$ of the accepted DT candidates are shown in the left column of Fig. 1. Signal events cluster around $M_{\text{BC}}^{\text{tag}} = M_{\text{BC}}^{\text{sig}} = M_{D^+}$, where M_{D^+} is the known D^+ mass. [1]. There are three kinds of background events. The events with correctly reconstructed D^+ (D^-) and incorrectly reconstructed D^- (D^+) are called BKGI. These background events are distributed along the horizontal and vertical bands around the nominal D^+ mass. The events spreading along the diagonal, which are mainly from the $e^+e^- \rightarrow q\bar{q}$ processes, are named BKGII. The events with incorrectly reconstructed D^- and D^+ are attributed to BKGIII and they are dispersed in the allowed kinematic region.

The signal yields of the DT events are extracted from a two-dimensional (2D) unbinned maximum likelihood fit to the corresponding distribution of $M_{\text{BC}}^{\text{tag}}$ versus $M_{\text{BC}}^{\text{sig}}$. The signal shape is described by the 2D probability density function (PDF) from the MC simulation. For various background components, the individual PDFs are constructed as [2, 30]

- BKGI: $b(x) \cdot c_y(y; E_b, \xi_y) + b(y) \cdot c_x(x; E_b, \xi_x)$,
- BKGII: $c_z(z; \sqrt{2}E_b, \xi_z) \cdot g(k; 0, \sigma_k)$,
- BKGIII: $c_x(x; E_b, \xi_x) \cdot c_y(y; E_b, \xi_y)$.

Here, $x = M_{\text{BC}}^{\text{tag}}$, $y = M_{\text{BC}}^{\text{sig}}$, $z = (x + y)/\sqrt{2}$, and $k = (x - y)/\sqrt{2}$. The one-dimensional MC-simulated signal shapes are $b(x)$ and $b(y)$. For background, c_f with $f \equiv x, y, \text{ or } z$ is an ARGUS function [31] defined as

$$c_f(f; E_{\text{end}}, \xi_f) = A_f f \left(1 - \frac{f^2}{E_{\text{end}}^2}\right)^{\frac{1}{2}} e^{\xi_f \left(1 - \frac{f^2}{E_{\text{end}}^2}\right)}, \quad (2)$$

where A_f is a normalization factor, ξ_f is a fit parameter, and E_{end} is the endpoint fixed at E_b for c_x and c_y or $\sqrt{2}E_b$ for c_z . The function $g(k; 0, \sigma_k)$ is a Gaussian

function with zero mean and standard deviation $\sigma_k = \sigma_0 \cdot (\sqrt{2}E_b - z)^p$, where σ_0 and p are the parameters determined from the fit. The BKGIII component is neglected because of limited statistics. All parameters are free in the fit. The spectra of the middle and right columns in Fig. 1 show the projections on $M_{\text{BC}}^{\text{tag}}$ and $M_{\text{BC}}^{\text{sig}}$ of the 2D fits to data. These fits give the signal yields of $D^+ \rightarrow K^+\pi^0\pi^0$ and $D^+ \rightarrow K^+\pi^0\eta$ to be $34.4 \pm 6.4_{\text{stat}}$ and $15.4 \pm 4.4_{\text{stat}}$, respectively.

The efficiency of detecting the signal decay $D^+ \rightarrow K^+\pi^0\pi^0(\eta)$ is estimated by using an admixture of the signal MC events for the resonant decay $D^+ \rightarrow K^{*+}\pi^0(\eta)$ and the phase space decay $D^+ \rightarrow K^+\pi^0\pi^0(\eta)$. The fractions of $D^+ \rightarrow K^{*+}\pi^0(\eta)$ ($r_{K^{*+}\pi^0(\eta)}$) are determined in the next paragraph. The signal yield of the resonant decay $D^+ \rightarrow K^{*+}\pi^0(\eta)$ is extracted from a simultaneous 2D fit to the DT candidate events when the $K^+\pi^0$ invariant mass ($M_{K^+\pi^0}$) lies in the K^{*+} signal and sideband regions, whose definitions are shown in Fig. 2.

The left columns of Figs. 3(a) and 3(b) show the $M_{\text{BC}}^{\text{tag}}$ versus $M_{\text{BC}}^{\text{sig}}$ distributions of the accepted DT candidates, where the top and bottom rows correspond to the K^{*+} signal and sideband regions, respectively. In the simultaneous fits, the ratios of the phase space background yield in the K^{*+} sideband region relative to that in the K^{*+} signal region are fixed to the MC-determined values of $f_{K^{*+}\pi^0} = 1.40 \pm 0.02$ for $D^+ \rightarrow K^+\pi^0\pi^0$ and $f_{K^{*+}\eta} = 2.25 \pm 0.05$ for $D^+ \rightarrow K^+\pi^0\eta$, respectively. These factors include the difference of phase space and efficiencies in the K^{*+} signal and sideband regions. From these fits, we obtain the signal yields of $D^+ \rightarrow K^{*+}\pi^0$ and $D^+ \rightarrow K^{*+}\eta$, $10.4^{+5.7}_{-5.3_{\text{stat}}}$ and $9.8^{+4.0}_{-3.4_{\text{stat}}}$, respectively. These give $r_{K^{*+}\pi^0} = 0.30 \pm 0.17_{\text{stat}}$ and $r_{K^{*+}\eta} = 0.64 \pm 0.30_{\text{stat}}$.

The statistical significance is evaluated using $\sqrt{-2\ln(\mathcal{L}_0/\mathcal{L}_{\text{max}})}$, where \mathcal{L}_{max} is the maximum likelihood of the nominal fit and \mathcal{L}_0 is the likelihood of the fit excluding the signal PDF. The resulting significances are 8.0σ , 5.0σ , 1.9σ , and 3.3σ for $D^+ \rightarrow K^+\pi^0\pi^0$, $D^+ \rightarrow K^+\pi^0\eta$, $D^+ \rightarrow K^{*+}\pi^0$, and $D^+ \rightarrow K^{*+}\eta$, respectively.

The measured values for N_{DT} , ϵ_{sig} , and \mathcal{B}_{sig} are summarized in Table 1. Because there is no significant signal for $D^+ \rightarrow K^{*+}\pi^0$, we set an upper limit on its decay BF at the 90% confidence level to be 4.5×10^{-4} . This is set utilizing the Bayesian approach after incorporating the associated systematic uncertainty [32], as discussed later.

One of the advantages of the DT method is that most of the uncertainties associated with the ST selection cancel. The systematic uncertainties in the BF measurements are mainly from the following sources. They are reported relative to the measured BFs. The uncertainty of the total ST D^- yield, which is mainly due to the fit to the $M_{\text{BC}}^{\text{tag}}$ distribution, is 0.5% [20–

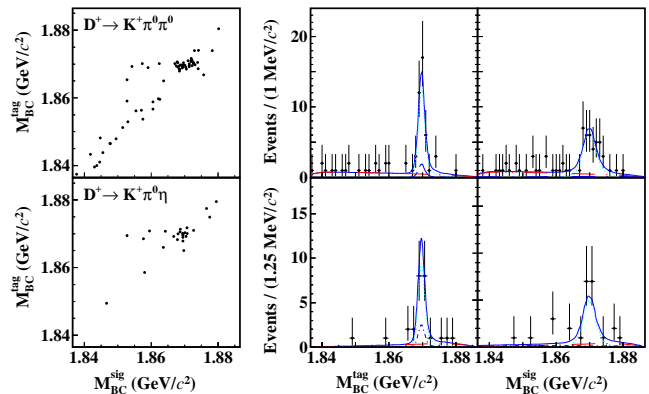


Fig. 1. Distributions of (left column) $M_{\text{BC}}^{\text{tag}}$ versus $M_{\text{BC}}^{\text{sig}}$ and the projections on (middle column) $M_{\text{BC}}^{\text{tag}}$ and (right column) $M_{\text{BC}}^{\text{sig}}$ of the 2D fits to the DT candidate events. The top row is for $D^+ \rightarrow K^+\pi^0\pi^0$ and the bottom row is for $D^+ \rightarrow K^+\pi^0\eta$. Points with error bars are data. Blue solid curves are the fit results. Cyan dotted curves are the fitted signal distributions. Blue dot-dashed curves are BKG I. Red dot-long-dashed curves are BKG II.

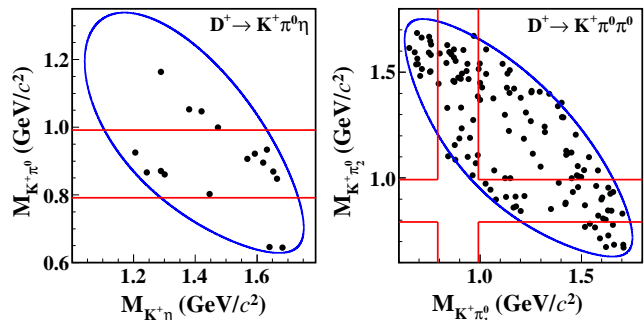


Fig. 2. Distributions of (left) $M_{K^+\eta}$ versus $M_{K^+\pi^0}$ for $D^+ \rightarrow K^+\pi^0\eta$ candidates and (right) $M_{K^+\pi^0}$ versus $M_{K^+\pi^0^2}$ for $D^+ \rightarrow K^+\pi^0\pi^0$ candidates. The π_1^0 and π_2^0 are labelled randomly. In the kinematic region marked in blue, the regions inside and outside the red band are the K^{*+} signal and sideband regions, respectively. Red bands correspond to ± 100 MeV/ c^2 around the known K^{*+} mass. The requirement of $|M_{\text{BC}}^{\text{tag(sig)}} - M_{D^+}| < 0.005$ GeV/ c^2 has been imposed.

Table 1. The DT yields in data (N_{DT}), the signal efficiencies ($\epsilon_{\text{sig}} = \epsilon_{\text{DT}}^i / \epsilon_{\text{ST}}^i$) and the obtained BFs. The first and second uncertainties are statistical and systematic, respectively. The efficiencies do not include the BFs of η and K^{*+} decays. The lower efficiency for $D^+ \rightarrow K^+\pi^0\pi^0$ is mainly due to the K_S^0 rejection.

Decay mode	N_{DT}	ϵ_{sig} (%)	$\mathcal{B}_{\text{sig}} (\times 10^{-4})$
$D^+ \rightarrow K^+\pi^0\pi^0$	34.4 ± 6.4	18.22 ± 0.04	$2.1 \pm 0.4 \pm 0.1$
$D^+ \rightarrow K^+\pi^0\eta$	15.4 ± 4.4	20.66 ± 0.04	$2.1 \pm 0.6 \pm 0.1$
$D^+ \rightarrow K^{*+}\pi^0$	$10.4^{+5.7}_{-5.3}$	14.18 ± 0.04	$2.5^{+1.4}_{-1.3} \pm 0.1$
$D^+ \rightarrow K^{*+}\eta$	$9.8^{+4.0}_{-3.4}$	17.78 ± 0.07	$4.7^{+1.9}_{-1.6} \pm 0.2$

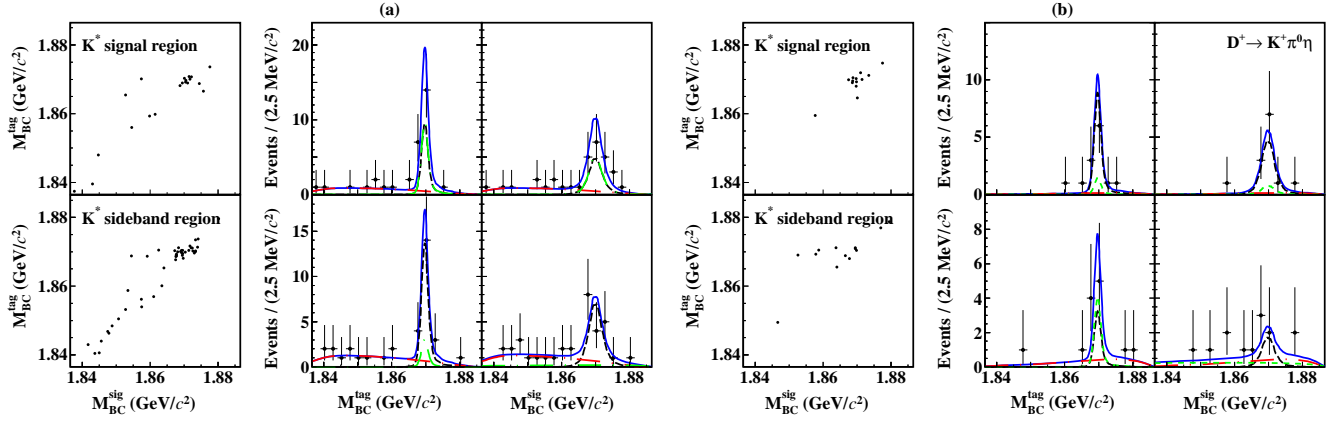


Fig. 3. Distributions of (left column) M_{BC}^{tag} versus M_{BC}^{sig} and the projections on (middle column) M_{BC}^{tag} and (right column) M_{BC}^{sig} of the constrained 2D fits to the DT candidate events in the K^* signal region (top row) and sideband region (bottom row) for (a) $D^+ \rightarrow K^+\pi^0\pi^0$ and (b) $D^+ \rightarrow K^+\pi^0\eta$. Points with error bars are data. Blue solid curves are the fit results. Black dotted curves are the signal distributions. For the K^* sideband region, green dotted and red dot-long-dashed curves are BKGII and BKGII, respectively. For the K^* signal region, red dot-long-dashed curves are BKGII and green dotted curves are the peaking backgrounds constrained by using the K^* sideband events.

[22]. The efficiencies of tracking and particle identification of the K^+ are studied with DT $D\bar{D}$ hadronic events. The systematic uncertainty for K^+ tracking is 1.0%. The efficiency of π^0 reconstruction is investigated using DT $D\bar{D}$ hadronic decay samples of $D^0 \rightarrow K^-\pi^+\pi^+$, $K^-\pi^+\pi^+\pi^-$ versus $\bar{D}^0 \rightarrow K^+\pi^-\pi^0$, $K_S^0\pi^0$ [20, 21]. The systematic uncertainty due to π^0 reconstruction is 2.0%. Based on the π^0 uncertainty, the systematic uncertainty of η reconstruction is also taken to be 2.0%. The uncertainties on the quoted BFs of $\eta \rightarrow \gamma\gamma$ and $\pi^0 \rightarrow \gamma\gamma$ are 0.5% and 0.03% [1], respectively.

The systematic uncertainty of the 2D fit is estimated by varying the signal and background shapes. The signal shape is varied by convolving with a Gaussian resolution function with parameters derived from a control sample of $D^+ \rightarrow \pi^+\pi^0\pi^0$. For the background, the endpoint of the ARGUS function is varied by ± 0.2 MeV/ c^2 . Adding the changes of the BFs quadratically gives corresponding systematic uncertainties of 1.5% for $D^+ \rightarrow K^+\pi^0\pi^0$ and 2.9% for $D^+ \rightarrow K^+\pi^0\eta$, but are negligible for $D^+ \rightarrow K^{*+}\pi^0$ and $D^+ \rightarrow K^{*+}\eta$.

The systematic uncertainty arising from the requirement of the D^+D^- opening angle is assigned to be 1.2% using a control sample of $D^+ \rightarrow \pi^+\pi^0\pi^0$. The systematic uncertainty of the ΔE_{sig} requirement is estimated by smearing one Gaussian resolution function obtained from the control sample with the ΔE_{sig} distribution of the signal MC events. The change of the DT efficiency is found to be negligible. Therefore, the corresponding systematic uncertainty is neglected. The systematic uncertainty due to the K_S^0 rejection is also negligible since the BFs are found to be insensitive to shrinking or enlarging the K_S^0 rejection window by 0.02 GeV/ c^2 and

taking into account correlations of the two signal samples with the nominal and varied K_S^0 signal regions [33].

The systematic uncertainty of the K^{*+} signal region is studied using DT events from the processes $D^0 \rightarrow K^-\pi^+\pi^+$ and $K^-\pi^+\pi^0$ versus $\bar{D}^0 \rightarrow K^{*+}(\rightarrow K^+\pi^0)e^-\bar{\nu}_e$. The change of the DT efficiencies after smearing the obtained Gaussian resolution function with the $M_{K^+\pi^0}$ distributions, 0.1%, is assigned as the associated uncertainty. The uncertainties of MC statistics are 0.2%, 0.2%, 0.3%, and 0.4% for $D^+ \rightarrow K^+\pi^0\pi^0$, $D^+ \rightarrow K^+\pi^0\eta$, $D^+ \rightarrow K^{*+}\pi^0$, and $D^+ \rightarrow K^{*+}\eta$, respectively. The systematic uncertainties related to the MC modeling for $D^+ \rightarrow K^+\pi^0\pi^0$ and $D^+ \rightarrow K^+\pi^0\eta$ are estimated by varying $r_{K^{*+}\pi^0(\eta)}$ by $\pm 1\sigma$ and are assigned to be 2.1% and 1.6%, respectively. Variations of $f_{K^{*+}\pi^0}$ and $f_{K^{*+}\eta}$ by $\pm 1\sigma$ cause systematic uncertainties of 0.9% and 0.7% for $D^+ \rightarrow K^+\pi^0\pi^0$ and $D^+ \rightarrow K^+\pi^0\eta$, respectively. Adding the above effects in quadrature yields the total systematic uncertainty for each signal process. They are 5.1%, 5.6%, 4.5%, and 4.5% for $D^+ \rightarrow K^+\pi^0\pi^0$, $D^+ \rightarrow K^+\pi^0\eta$, $D^+ \rightarrow K^{*+}\pi^0$, and $D^+ \rightarrow K^{*+}\eta$, respectively.

To summarize, using 2.93fb^{-1} of e^+e^- annihilation data [12] taken at $\sqrt{s} = 3.773$ GeV, we report the first measurements of the BFs of the DCS decays $D^+ \rightarrow K^+\pi^0\pi^0$, $D^+ \rightarrow K^+\pi^0\eta$, $D^+ \rightarrow K^{*+}\pi^0$, and $D^+ \rightarrow K^{*+}\eta$, as summarized in Table 1. We do not observe significant signal for $D^+ \rightarrow K^{*+}\pi^0$ and thereby set the upper limit on the BF of this decay at the 90% confidence level to be 4.5×10^{-4} . Amplitude analyses of these decays with larger data samples in the future [34, 35] will supply more precise information about $D^+ \rightarrow K^{*+}\pi^0$ and $D^+ \rightarrow K^{*+}\eta$, and will be important for more detailed

investigations of SU(3) flavor symmetry breaking effects as well as for our understanding of CP violation phenomena in hadronic decays of charmed mesons. Using $\mathcal{B}_{D^+ \rightarrow K^- \pi^+ \pi^+} = (9.38 \pm 0.16)\%$ [1] and $\mathcal{B}_{D^+ \rightarrow K^+ \pi^+ \pi^-} = (4.91 \pm 0.09) \times 10^{-4}$ [1], we obtain the DCS/CF BF ratios $\mathcal{B}_{D^+ \rightarrow K^+ \pi^0 \pi^0} / \mathcal{B}_{D^+ \rightarrow K^- \pi^+ \pi^+} = (2.26 \pm 0.40) \times 10^{-3}$ and $\mathcal{B}_{D^+ \rightarrow K^+ \pi^0 \eta} / \mathcal{B}_{D^+ \rightarrow \bar{K}^0 \pi^+ \eta} = (8.09 \pm 2.13) \times 10^{-3}$. They correspond to $(0.78 \pm 0.14) \tan^4 \theta_C$ and $(2.79 \pm 0.64) \tan^4 \theta_C$, respectively, implying that no abnormal DCS/CF BF ratios are found.

The BESIII collaboration thanks the staff of BEPCII and the IHEP computing center for their strong support. This work is supported in part by National Key R&D Program of China under Contracts Nos. 2020YFA0406400 and 2020YFA0406300; National Natural Science Foundation of China (NSFC) under Contracts Nos. 11775230, 11625523, 11635010, 11735014, 11822506, 11835012, 11935015, 11935016, 11935018, 11961141012, 12022510, 12025502, 12035009, 12035013, 12061131003; the Chinese Academy of Sciences (CAS) Large-Scale Scientific Facility Program; Joint Large-Scale Scientific Facility Funds of the NSFC and CAS under Contracts Nos. U1732263, U1832207, U1932102; CAS Key Research Program of Frontier Sciences under Contract No. QYZDJ-SSW-SLH040; 100 Talents Program of CAS; INPAC and Shanghai Key Laboratory for Particle Physics and Cosmology; ERC under Contract No. 758462; European Union Horizon 2020 research and innovation programme under Contract No. Marie Skłodowska-Curie grant agreement No 894790; German Research Foundation DFG under Contracts Nos. 443159800, Collaborative Research Center CRC 1044, FOR 2359, FOR 2359, GRK 214; Istituto Nazionale di Fisica Nucleare, Italy; Ministry of Development of Turkey under Contract No. DPT2006K-120470; National Science and Technology fund; Olle Engkvist Foundation under Contract No. 200-0605; STFC (United Kingdom); The Knut and Alice Wallenberg Foundation (Sweden) under Contract No. 2016.0157; The Royal Society, UK under Contracts Nos. DH140054, DH160214; The Swedish Research Council; U. S. Department of Energy under Contracts Nos. DE-FG02-05ER41374, DE-SC-0012069.

[1] P. A. Zyla *et al.* (Particle Data Group), *Prog. Theor. Exp. Phys.* **2020**, 083C01 (2020).
 [2] M. Ablikim *et al.* (BESIII Collaboration), *Phys. Rev. Lett.* **125**, 141802 (2020).
 [3] M. Ablikim *et al.* (BESIII Collaboration), *Phys. Rev. D* **104**, 072005 (2021).
 [4] H. Y. Cheng and C. W. Chiang, *Phys. Rev. D* **81**, 074021

(2010).
 [5] F. S. Yu, X. X. Wang, and C. D. Lü, *Phys. Rev. D* **84**, 074019 (2011).
 [6] H. J. Lipkin, *Phys. Rev. Lett.* **46**, 1307 (1981).
 [7] Q. Qin, H. N. Li, C. D. Lü, and F. S. Yu, *Phys. Rev. D* **89**, 054006 (2014).
 [8] H. Y. Cheng, C. W. Chiang, and A. L. Kuo, *Phys. Rev. D* **93**, 114010 (2016).
 [9] W. Kwong and S. P. Rosen, *Phys. Lett. B* **298**, 413 (1993).
 [10] Y. Grossman and D. J. Robinson, *J. High Energy Phys.* **1304**, 067 (2013).
 [11] H. N. Li, C. D. Lü, and F. S. Yu, *Phys. Rev. D* **86**, 036012 (2012).
 [12] M. Ablikim *et al.* (BESIII Collaboration), *Chin. Phys. C* **37**, 123001 (2013); *Phys. Lett. B* **753**, 629 (2016).
 [13] M. Ablikim *et al.* (BESIII Collaboration), *Nucl. Instrum. Meth. A* **614**, 345 (2010).
 [14] S. Agostinelli *et al.* (GEANT4 Collaboration), *Nucl. Instrum. Meth. A* **506**, 250 (2003).
 [15] S. Jadach, B. F. L. Ward, and Z. Was, *Phys. Rev. D* **63**, 113009 (2001); *Comput. Phys. Commun.* **130**, 260 (2000).
 [16] D. J. Lange, *Nucl. Instrum. Meth. A* **462**, 152 (2001); R. G. Ping, *Chin. Phys. C* **32**, 599 (2008).
 [17] J. C. Chen, G. S. Huang, X. R. Qi, D. H. Zhang, and Y. S. Zhu, *Phys. Rev. D* **62**, 034003 (2000).
 [18] E. Richter-Was, *Phys. Lett. B* **303**, 163 (1993).
 [19] R. M. Baltrusaitis *et al.* (Mark III Collaboration), *Phys. Rev. Lett.* **56**, 2140 (1986); J. Adler *et al.* (Mark III Collaboration), *Phys. Rev. Lett.* **60**, 89 (1988).
 [20] M. Ablikim *et al.* (BESIII Collaboration), *Eur. Phys. J. C* **76**, 369 (2016).
 [21] M. Ablikim *et al.* (BESIII Collaboration), *Chin. Phys. C* **40**, 113001 (2016).
 [22] M. Ablikim *et al.* (BESIII Collaboration), *Phys. Rev. Lett.* **121**, 171803 (2018).
 [23] M. Ablikim *et al.* (BESIII Collaboration), *Phys. Rev. Lett.* **123**, 231801 (2019).
 [24] M. Ablikim *et al.* (BESIII Collaboration), *Phys. Rev. D* **101**, 052009 (2020).
 [25] M. Ablikim *et al.* (BESIII Collaboration), *Phys. Rev. D* **101**, 072005 (2020).
 [26] M. Ablikim *et al.* (BESIII Collaboration), *Phys. Rev. Lett.* **124**, 231801 (2020).
 [27] M. Ablikim *et al.* (BESIII Collaboration), *Phys. Rev. Lett.* **124**, 241803 (2020).
 [28] M. Ablikim *et al.* (BESIII Collaboration), *Phys. Rev. D* **102**, 052006 (2020).
 [29] M. Ablikim *et al.* (BESIII Collaboration), *Phys. Rev. D* **102**, 112005 (2020).
 [30] S. Dobbs *et al.* (CLEO Collaboration) *Phys. Rev. D* **76**, 112001 (2007).
 [31] H. Albrecht *et al.* (ARGUS Collaboration), *Phys. Lett. B* **241**, 278 (1990).
 [32] K. Stenson, arXiv:physics/0605236.
 [33] R. Barlow, arXiv:physics/0207026.
 [34] M. Ablikim *et al.* (BESIII Collaboration), *Chin. Phys. C* **44**, 040001 (2020).
 [35] H. B. Li and X. R. Lyu, arXiv:abs/2103.00908.